Peer-reviewed version available at *J. Compos. Sci.* **2020**, *4*, 118; doi:10.3390/jcs4030118

Article

Polymethylmethacrylate (PMMA) Encapsulated Graphene Oxide Nanocomposite: Pre-modification, Synthesis, and Latex Stability

Hui Wang [1,2,a], Letian Wang [2,a], Shanyu Meng [2], Hanxue Lin [1], Melanie Correll[2], and Zhaohui Tong [2,*]

[1] College of Material Science and Engineering, Central South University of Forestry and Technology, Changsha, China, 410004.
[2] Department of Agricultural and Biological Engineering, IFAS, University of Florida, Gainesville, FL, USA, 32611-0570
[*] Correspondence: ztong@ufl.edu
[a] These authors contributed equally in this work.

Abstract: The compatibility of graphene or graphene oxide with its dispersion medium (polymer) plays a critical role in the formation nanocomposite materials with significant property improvements. Environmentally friendly miniemulsion polymerization, which allows a formation of nanoencapsulation in an aqueous phase and high molecular weight polymer/composite production is one promising method. In this study, we screened a series of amphiphilic modifiers and found that the quaternary ammonium (ar-vinyl benzyl) trimethyl ammonium chloride (VBTAC) pending carbon double bonds could effectively modify the graphene oxide (GO) to be compatible with the organophilic monomer. After that, free radical miniemulsion polymerization could successfully synthesize stable latex of exfoliated poly (methyl methacrylate) (PMMA)/ GO nanocomposite. The final latex had an extended storage life and a relatively uniform particle size distribution. X-ray powder diffraction (XRD), transmission electron microscopy (TEM), and scanning electron microscopy (SEM) analysis of this latex and its films indicated successful encapsulation of exfoliated nano-dimensional graphene oxide inside a polymer matrix.

Keywords: graphene oxide; exfoliation; nanocomposites; encapsulation; stable latex

1. Introduction

Nanocomposites consisting of polymer and inorganic particles with a sub-micron scale, such as carbon black, carbon nanotubes, graphene, and nanoclay, have been extensively studied in the last decades because these materials possess superior mechanical, thermal, electric, or gas barrier properties [1-4]. Among these inorganic materials, graphene and graphene oxide (GO) have attracted interest since they can prepare various functional nanocomposites for different applications in the energy and environmental areas [5-9]. Along with its high thermal (up to 5000 w/(m.k.)) and electrical conductivity (up to 6000 S/cm), graphene is also an excellent candidate as a superior enforcement nanomaterial because it has strong mechanical properties with Young's modulus of approximately 1 TPa, the strength of 130 GPa [10-13] and high specific surface area when it is dispersed into the polymer matrix.

Graphite is a layered material consisting of stacked graphene sheets in parallel. It consists of six hexagonally arranged sp^2 hybridized carbon atoms in a 2-D sheet-like morphology with one atom thickness [14]. However, natural graphene sheets lack accessible functional groups on their surface for the polymer to be intercalated or loaded, this results in the incompatibility between polymer matrixes with the natural graphite sheet. But graphite can be easily converted to graphene oxide (GO) through oxidation [15-17], which provides multiple oxygen-containing functional groups on its

Peer-reviewed version available at J. Compos. Sci. 2020, 4, 118; doi:10.3390/jcs4030118

surface, such as hydroxyl, carboxyl, and epoxy groups. All these functional groups are crucial for the subsequent functionalization treatments, as well as the incorporation with polymers [18]. GO are in layered structures and its oxidative functionalities are located in the basal plane of the graphene sheet causing hydrophilicity, which results in exfoliation to the nanoscale platelet and dispersion in the aqueous phase [19]. Putz *et al*. (2010) described the dispersion of graphene nanosheets using a flow-through ultrasonication method followed by a vacuum-assisted self-assembly (VASA) technique to prepare highly ordered, homogeneous polymer nanocomposites with the layered graphene oxide using both hydrophilic and hydrophobic polymers[20]. GO and hydrophilic polymers can form homogeneous nanocomposites but possess weak and volatile mechanical properties because they can absorb water very easily. Poor interaction between the hydrophilic GO and the hydrophobic polymer is a major concern for preparing high-quality GO-based nanocomposites. Therefore, GO has been modified by an amine, an alkyl lithium reagent, isocyanate and di-isocyanate, amphiphilic polymers such as poly (sodium 4-styrene sulfonate), 7,7,8,8-tetracyanoquinodimethane, sulfonated polyaniline, and diazonium salt to be hydrophobic and amenable to different synthetic polymers. However, these methods including solution blending, bulk polymerization, and melt-intercalation [21-23] require the use of toxic organic solvents, high temperature, or produce the non-uniform distribution of the GO sheet in the polymer matrix.

It is known that nanocomposites in an aqueous form show many unique advantages over their bulk and solvent forms in terms of improved environmental impacts, energy-saving, and product control [3, 24]. To increase the compatibility between hydrophilic GO sheet with organophilic polymers, the oil-in-water system has been adapted to resolve this incompatibility issue as well as to avoid the use of environmentally harmful organic solvents. For example, Thomassin *et al.* (2014) found that GO served as the surfactant and adsorbed on the PMMA surface through the precipitation polymerization process in a water/methane mixture [25]. Wang *et. al* (2004) described a method to intercalate GO into a monomer solution followed by *in-situ* emulsion polymerization for the production of the poly (methyl methacrylate) (PMMA)/GO composite. The results showed that mechanical properties decreased with the increase of the ratio of GO because GO was not fully exfoliated into a nanometer scale [26]. Graphene-polystyrene (PS) nanocomposite with high electrical conductivity have been successfully synthesized via emulsion polymerization followed by a GO reduction reaction using hydrazine hydrate. The PS particles were linked with GO edges, which increased the organophilic property of GO [27]. GO or RGO (reduced graphene oxide) nanocomposites have been studied via various oil-in- water systems including ultrasonic-assisted in-situ emulsion polymerization [28], microemulsion polymerization[29], in-situ seed emulsion polymerization[30], picking emulsion polymerization[31], reversible addition fragment chain transfer (RAFT) emulsion polymerization [32], surfactant free emulsion polymerization followed by electrostatic interaction methods [33]. These nanocomposites have high conductivity and can also serve as coating materials to encapsulate phase change materials. Improvements on the distribution of GO or RGO in the polymer matrix could lower the percolation threshold and provide greater electrical conductivities [34]. In these aforementioned colloidal latex systems, polymer particles are usually attached on the edge of the GO sheet or the GO sheets are coated on their surface, which impede the aggregation of the GO sheets. However, in these colloidal latex systems such as emulsion, precipitation, and macroemulsion, the GO sheets are randomly separated by the polymer particles instead of the formation of a highly ordered and fully exfoliated nanoscale dispersion in the polymer matrix. The incompatibility between the hydrophilic GO and the hydrophobic polymer still requires further improving due to the weak intercalation of the polymer nanoparticles into the graphene base plane.

Miniemulsion has the advantages over emulsion polymerization in the synthesis of stable nanocomposite latex. The loci of polymerization for the miniemulsion is the monomer droplets instead of micelles in emulsion which avoids mass transfer and enables the filler encapsulation by polymer droplets [35, 36]. This method produces not only stable latex of nano-droplets with the diameter of 50 – 500 nm and narrow particle size distribution, but also nanocomposites with high molecular weight because the bimolecular termination is suppressed [37]. Miniemulsion

Peer-reviewed version available at J. Compos. Sci. 2020, 4, 118; doi:10.3390/jcs4030118

polymerization has been extensively studied to intercalate inorganic particles such as nanoclay, carbon black, carbon nanotubes, TiO_2 into the polymer matrix [3, 4, 38] to form uniform and stable latex of nanocomposites with the improved mechanical, thermal and barrier properties. A few researchers have also synthesized the GO or graphene-based nanocomposites via miniemulsion polymerization. For example, nano-dimensional GO sheets were armored on the polystyrene nanoparticles via a miniemulsion polymerization but the reduction occurred during polymerization resulting in the loss of colloidal stability[39]. This method has also been applied to prepare hollow hybrid polymer/GO nanoparticles [31, 39-41] and GO was coated on the surface but not encapsulated into polymer nanoparticles. A few researchers described for the synthesis of exfoliated GO/polymer nanocomposites prepared with pre-modified GO via miniemulsion polymerization using a reactive surfactant, 2-acrylamido-2-methyl-1-propanesulfonic acid (AMPS)[19], poly(ionic liquid) (PIL)[42], and r-methacryloxypropyl trimethoxy silane (MPS)[43]. The monomer type, the addition of conventional surfactant, pH value and ionic strength, have proved to affect the polymerization kinetics, latex stability, nanocomposite properties, and the intercalation degree for both traditional miniemulsion polymerization or picking miniemulsion polymerization [40, 44, 45]. In miniemulsion polymerization, the modifiers have shown their effectiveness to prepare exfoliated polymer encapsulated GO nanocomposite latex. However, it is unclear how different modifiers could affect the compatibility between the GO and the organophilic monomer, the latex stability, the reaction kinetics, and the exfoliation and encapsulation degree.

In this study, GO was prepared from a low cost, bulk, raw graphite via a modified Hummers' method [46]. Then, we used different amphiphilic modifiers to not only intercalate into the graphene platelet but also transfer GO from hydrophilic to organophilic. The modifiers included the reactive surfactant (ar-vinyl benzyl) trimethyl ammonium chloride (VBTAC), 2-acrylamido-2-methyl-1-propane sulphonic acid (AMPS), traditional surfactant sodium dodecylbenzene sulfonate (SDBS), surfactants with different carbon chains (octadecyl trimethylammonium bromide OTAB, trimethyl(tetradecyl) ammonium bromide (MTAB), and an amphiphilic modifier derived with highly crosslinked polymer lignin (quaternary ammonium lignin, QAL)[47, 48]. GO was modified with these modifiers and then dispersed in the oil/water system. The stability and distribution of the modified GO on the oil/water system determined the optimized GO modifier for further miniemulsion polymerization. After that, we conducted miniemulsion polymerization to synthesize stable latex with a PMMA encapsulated the nano-dimensional and exfoliated GO sheet. The uniform distribution of exfoliated GO in this system is expected to achieve significant property improvement and stable latex will benefit for long-term storage.

2. Materials and Methods

2.1. Materials

The lignin was extracted from the fermentation broth of a bioethanol process, which involves liquefaction plus simultaneous saccharification and fermentation process (L+SScF) using sugarcane bagasse as raw materials [49]. Raw graphite flake with an average size of 20 μm was purchased from Sigma-Aldrich Inc. (U.S.A.) and used as received. Monomer methyl methacrylate (MMA), 99%, was purchased from Sigma-Aldrich Inc. (U.S.A.), the inhibitor (monomethyl ether hydroquinone) was removed by passing through a glass column filled with aluminum oxide powder. (Vinyl benzyl) trimethyl ammonium chloride (VBTAC, 99%), 2-acrylamido-2-methyl-1-propane sulphonic cid (AMPS), sodium dodecylbenzene sulfonate (SDBS, technical grade), Triton 405 (TX-405, 70% solution in water), hexadecane (HD, 99%), 2,2'-Azoisobutyronitrile (AIBN, 98%), 4-methoxyphenol (99%), were all purchased from Sigma-Aldrich Inc. (U.S.A.) and used as received. Polyvinyl alcohol (PVA, 99%, Mw = 86000) granules, trimethylamine (TMA, 50% aqueous solution), and epichlorohydrin (ECH, 99%) were purchased from Acros Organics (Thermo Fisher Scientific, NJ, U.S.A.). Sulfuric acid (98%), potassium permanganate (99%) and hydrogen peroxide (30%) were purchased from Fisher Scientific (U.S.A.) and used as received. Silver nitrate (0.025 M), was purchased from Ricca Chemicals (U.S.A.). Quaternary Ammonium Lignin (QAL) was synthesized according to our previous study[48].

Peer-reviewed version available at J. Compos. Sci. 2020, 4, 118; doi:10.3390/jcs4030118

2.2. Experiments

2.2.1. Preparation of graphene oxide (GO)

GO was prepared according to the modified Hummers Method [46]. In an ice bath, powdered flake graphite (10 g) and sodium nitrate (5 g) were added to 98% sulfuric acid (230 mL) in a 1.5 L flask that was previously cooled to -5 °C in a freezer. Potassium permanganate (30 g) was slowly added in a stirred suspension while the mixture temperature carefully remained below 20 °C. The ice bath was then removed, and the mixture was heated to 35°C and kept at that temperature for 30 min. Deionized water (460 mL) was then slowly added to the mixture, causing an increase in temperature to about 100 °C. The diluted mixture was maintained at 100 °C for 15 min before it was further diluted with warm deionized water (420 mL) and hydrogen peroxide (3%, 100 mL). The yellow-brownish GO was separated by a vacuum filtration process then washed repeatedly with deionized water until the effluent became neutral. GO was then re-dispersed in water and freeze-dried (Freeze Dryer 8, Labconco, MO, U.S.A.) to preserve its original structure and property for further use.

2.2.2. Pre-modification of GO

To further exfoliate the GO, the GO (before any further treatments) was dispersed in deionized water to form a suspension at a concentration of 1 wt.%. Ultrasonication was applied to the suspension in an ultrasonic homogenizer with the energy equivalent of 1.35 kWh, the power of 300V, and at a power setting of 90% and a pulse setting of 90% (BioLogics, Inc., VA, U.S.A.) in an ice bath. After sonication, a certain amount of the modifiers including VBTAC, MPS, SDBS, OTAB, MTAB, and QAL was added to the GO suspension and the concentration of each modifier was kept at 20 wt. % based on the GO weight. The suspension was stirred for 24 hrs to allow the modification reaction between each modifier and GO. The modified GO suspensions were observed at room temperature (23°C) to determine its solubility in water. Several modified GO suspensions were further dispersed into the monomer or monomer/water mixture to determine their stability in each solvent. For example, VBTAC treated GO suspension was dialyzed in deionized water (3.5 kD dialysis tube, Spectrum Laboratories, INC, TX, U.S.A.) until no chlorine could be detected by silver nitrate (about 3-4 days). After that, the modified GO samples were freeze-dried (Freeze Dryer 8, Labconco, MO, U.S.A.) to preserve their original structure and property.

2.2.3. Miniemulsion polymerization of methyl methacrylate (MMA) in the presence of graphene oxide (GO)

In a typical run (recipe in Table 1), the oil phase composed of 0.5 g of co-stabilizer hexadecane, 0.1 g of AIBN, 6 g of monomer MMA, and varying quantities of GO was mixed and then magnetically stirred for 30 min. The mixture was ultrasonicated in an ice bath for 3 min using an ultrasonic homogenizer (300V, BioLogics, Inc., VA, U.S.A.) at an energy equivalent of 0.27 kWh and on a 90% power and 90% pulse setting. The water phase mixture composed of 0.17g of TX-405, various amounts of PVA, was magnetically stirred in an ice bath for 30 min. PVA was used as a co-stabilizer to improve latex stability. The monomer phase was then transferred to the water phase, the mixture was then ultrasonicated again using the ultrasonic homogenizer with the energy equivalent of 0.08 kWh and on a 90% power and 90% pulse setting. The obtained miniemulsion was transferred into a three-neck flask equipped with a condenser, a mechanical overhead stirrer, and a temperature control unit. The miniemulsion was stirred for another 30 min at room temperature and degassed with nitrogen. The polymerization was then initiated by increasing the temperature to 70 ± 2 °C and the reaction was allowed to taken place for 8 hrs under continuous mechanical stirring. Upon 8 hrs. reaction, several drops of 2% 4-methoxy phenol were added to terminate the polymerization.

Table 1. A basic recipe for the synthesis of PMMA/GO nanocomposite latex via miniemulsion polymerization.

Peer-reviewed version available at J. Compos. Sci. 2020, 4, 118; doi:10.3390/jcs4030118

Mixtures	Component	Amount Added (g)	Percentage/ total (wt.%)	Percentage/ Monomer (wt.%)
Oil Phase	Methyl Methacrylate	6	20.00%	100.00%
	Hexadecane	0.5	1.67%	8.33%
	AIBN	0.1	0.33%	1.67%
	Poly Vinyl Alcohol (10% solution)	0.6	2.00%	10.00%
Water Phase	Triton-405	0.17	0.57%	2.83%
	Deionized Water	24	80.00%	400.00%

2.3. Characterization

Fourier transform infrared spectrometry (FTIR) spectra were recorded on a Thermo Nicolet Magna 760 FTIR spectrometer (Thermo Scientific, MA, U.S.A.). Each sample (0.1-2 mg) was mixed with 160 mg potassium bromide to prepare a pellet form ready for the FTIR measurement. Each sample were taken for 32 scans and in the scanning range from 400 to 4000cm^{-1} and at a resolution of 4.

X-Ray Diffraction (XRD) measurements were performed on a Phillips XPert MRD instrument (PANalytical, Almelo, The Netherlands) with Cu K radiation source (λ = 1.54056 Å) and at a voltage of 45 V, step size of 0.016°, scan step time of 5 s, scan angle from 5° to 60°. The d (001) basal - spacing of the raw graphite, GO, and the polymerized composite were calculated using the Bragg equation: $d = \lambda/2 \sin \theta$. Where d is the interlayer distance, λ is the wavelength of the X-Ray source (Cu K-alpha, λ = 0.15418 nm), θ is the diffraction angle.

The molecular weight (Mw) of the PMMA and its nanocomposites with GO together was measured by a size exclusion chromatography (SEC) via an Agilent Technologies 1260 series HPLC system equipped with a refractive index detector (RID) and a multiple wavelength detector (MWD) (CA, USA). Three columns (Agilent Technologies, CA, USA) were connected in series, including a PLgel-mixed B, a PLgel-mixed E (5 μm with a pore size of 10,000 Å), and a PLgel-mixed E (5 μm with a pore size of 100 Å). All samples were dissolved in HPLC-grade tetrahydrofuran at a concentration of 0.2 wt. %. After that, solution was filtered through a 0.22 μm syringe filter. In each run, 50 μL filtered solution was injected, the thermostat temperature and flow rate were set at 25 °C and 1 mL/min, respectively. All results were processed using ChemStation software with the GPC analysis package (Rev.B.04.03). Molecular weight was calculated based on a universal calibration using a set of polystyrene standards.

Thermogravimetric analysis (TGA) was performed using a Mettler Toledo (OH, U.S.A.) thermal analyzer. For each sample, 3-10 mg sample was heated at a heating rate of 10 °C/min from 30 to 1000 °C and in a constant nitrogen flow of 100 mL/min.

Dynamic light scattering (DLS) was used to estimate the size and size distribution of the GO samples and the miniemulsions after polymerization. A zeta sizer with noninvasive backscatter under 500 MW and 532 nm laser (ZS3600, Malven, U.K.) was used. All samples at a concentration of 0.05 or 0.1% were transferred to the standard 3.5 mL square cuvettes for the analysis.

Scanning electron microscopy (SEM) and transmission electron microscopy (TEM) were used to study the morphologies of graphite, GO, polymerized particles in miniemulsion, and the melting latex films. SEM was carried out on a FEI XL 40 FEG SEM (FEI instruments, OR, U.S.A.) at an operation voltage of 10 keV. Miniemulsion sample was dried on a conductive carbon tab then coated with a gold-palladium coating (Au/Pd). TEM was conducted on a JEOL 200CX TEM (JEOL instruments, MA, U.S.A.) with a 100 keV accelerating voltage. Miniemulsion samples were dried on carbon type A grids and air-dried prior to analysis. Melt film samples were dried in air and melt at 160 °C in a laboratory oven for 6 hrs.

3. Results

Peer-reviewed version available at *J. Compos. Sci.* **2020**, *4*, 118; doi:10.3390/jcs4030118

3.1. Modification of GO using different modifiers

To facilitate the encapsulation and exfoliation of GO into polymer droplets, It is a critical step that GO is well dispersed into the monomer phase before miniemulsion polymerization. Figure 1 shows the stability of the neat GO and the modified GO treated by different modifiers in water. It was observed that GO modified with AMPS (c) and SDBS (d) behaved quite similarly as the neat GO (a), which had good dispersibility in water. The oxidation reaction to convert graphene to GO, as expected, introduced functional groups such as COOH, OH on its surface, therefore, GO had good water dispersibility. But the GO treated with VBTAC (b), OTAB (e), and MTAB (f) precipitated out of the solution, which indicated that water-soluble functional groups on the GO surface were occupied by these modifiers and the modified GO were converted from hydrophilic to organophilic. This was likely caused by the fact that cationic quaternary ammonium end groups of VBTAC, OTAB, and MTAB modifiers were bound to the negative functional groups on the GO sheet surface. We also observed that OTAB (C18) and MTAB (C14) could significantly increase the viscosity of GO/monomer mixture, which impeded the dispersion into the aqueous phase in the following miniemulsion step and possibly reduced the polymerization rate [3]. Only VBTAC with a short phenolic structure had an acceptable viscosity for further dispersion into a stable miniemulsion.

We further introduced another cationic quaternary ammonium modifier (QAL) that was prepared from our lab. QAL was produced by reacting lignin with epoxypropyl trimethylammonium chloride (ETAC) and carried a crosslinking phenolic backbone structure and cationic quaternary ammonium end groups. SDBS was used as a comparison because it was an anionic surfactant that was reported to provide electrostatic stabilization for GO [50, 51]. Figure 2 shows the dispersion of the modified GO in the monomer/ water mixture using VBTAC, SDBS, and QAL. Since MMA had a lower density (0.94 g/cm^3) than water, it stayed afloat on the aqueous phase. It was clearly shown that only VBTAC modified GO stayed on the monomer MMA phase, the SDBS modified GO occupied in both water and monomer phases. Surprisingly, the QAL modified GO remained in the water phase. The network phenolic backbone structure might inhibit the contact between the cationic quaternary ammonium groups and the GO functional groups. Therefore, VBTAC was chosen for the modifier because it not only converted GO from hydrophilic to organophilic but also owned the reactive acrylic groups, which allowed further combination with the monomer MMA together during miniemulsion polymerization.

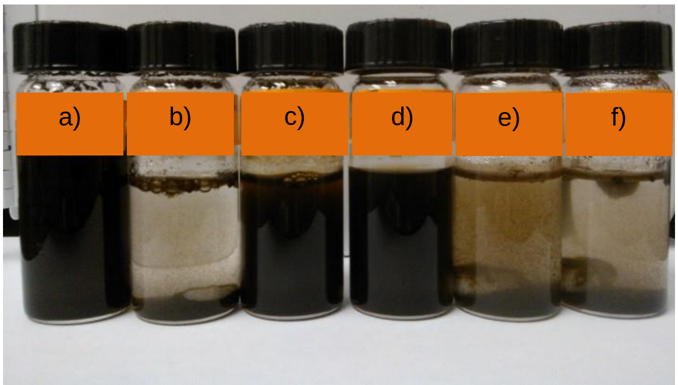

Figure 1. The visual appearance of 0.02 g GO and GO treated with 0.01 g different modifiers in the deionized water, 10 minutes after agitation was stopped, a) neat GO, b) GO with VBTAC, c) GO with AMPS, d) GO with SDBS, e) GO with OTAB, f) GO with MTAB.

Peer-reviewed version available at J. Compos. Sci. 2020, 4, 118; doi:10.3390/jcs4030118

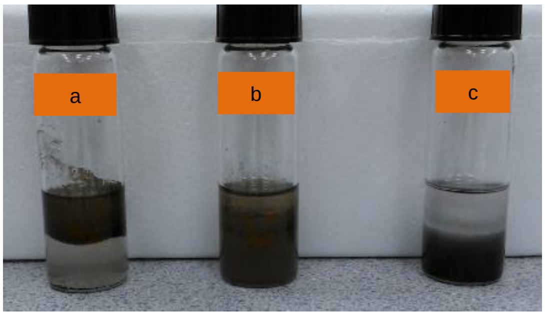

Figure 2. Visual appearance of 0.02 g GO with different modifiers in the MMA/water (50/50 v/v) mixture, 10-minute sitting after sonication, a) VBTAC, b) SDBS, c) QAL.

3.2. Fourier Transform Infrared Spectrometry (FTIR)

FTIR was used to confirm the chemical shift of the graphite, GO, reduced GO, and VBTAC-modified GO. As shown in Figure 3, GO had the represented peaks including the stretching vibration of carboxyl groups (-COOH) around 1700 cm^{-1} (a), the vibration of in-plane tertiary hydroxyl groups (-OH) at 1400 cm^{-1} (b) and the vibration of alkoxy (C-O) around 1050 cm^{-1} (c) in comparison with the graphene. It indicated that the original graphite was highly oxidized and functional groups such as COOH, OH were successfully added on the GO planes [52-55]. The new peak around 1600 cm^{-1} (d) of the carbon double bond C=C stretching was observed in the VBTAC modified GO, which provided the evidence for the successful combination of VBTA with the GO [3].

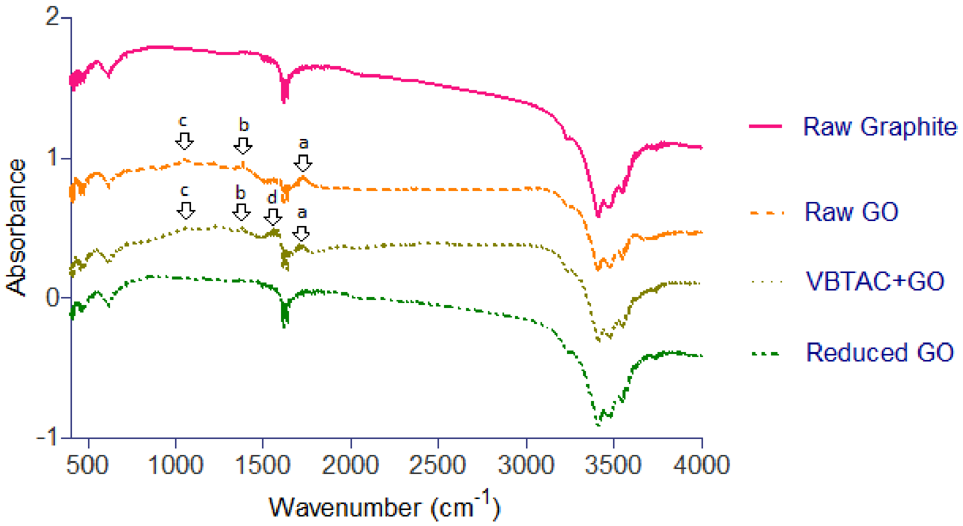

Figure 3. FTIR spectra of raw graphite, GO, reduced GO and VBTAC modified GO.

3.3. X-Ray Diffraction (XRD)

XRD was used to determine the interlayer spacing (d) of the GO and its composite samples. The d-spacing was calculated according to the Bragg equation: d = λ/2 sin θ. As shown in Figure 4, the spectra of raw graphite had a very strong characteristic peak at 2θ = 26.5°(interlayer spacing of 0.336 nm, the (002) structure) [56, 57]. The oxidation of graphite was expected to increase this interlayer distance (d-spacing). After oxidation, the diffraction curve of GO had a peak at 2θ = 11°, which denoted an interlayer spacing of 0.803 nm. The addition of oxygen containing groups and water molecules into the interlayer space between graphene sheets resulted in the expanding of the interlayer spacing during the GO preparation process. It was also observed that the strong characteristic peak at 2θ = 26.5° entirely disappeared, which indicated the complete disruption of the original stacked (002) structure of raw graphite [57]. The results from both XRD and FTIR provided strong evidence for the formation of the intercalated GO with oxidized functional groups. The cationic ammonium groups of VBTAC was designed to further enter the interlayer space of GO and

Peer-reviewed version available at J. Compos. Sci. 2020, 4, 118; doi:10.3390/jcs4030118

bonded with the negative oxidized functional groups of the GO sheets. Figure 4 also showed that the VBTAC-modified GO had a shifted peak from 2θ = 11˚ to approximate 2θ = 9˚ (d-spacing of 0.981), indicating that the interspacing of GO was further improved by VBTAC.

After miniemulsion polymerization, the diffraction peaks of the XRD spectra of the nanocomposite samples were quite different from the GO samples. As shown in figure 4 (below curves), the peaks at 9˚ and 11˚ corresponding to the GO and the VBTAC modified GO disappeared completely, indicating that the GO was completely exfoliated by the polymer chains. Similar phenomena were shown for nanoclay composites [3, 58]. The pure polymer PMMA had a characteristic peak at 18.5˚ [59], which became much less intensive and shifted to around 17.5˚ in the formulations with 0.5% and 2% GO. This further provided the evidence for the successful exfoliation of GO in the polymer matrix, leading to the disappearance or change of the original PMMA structure.

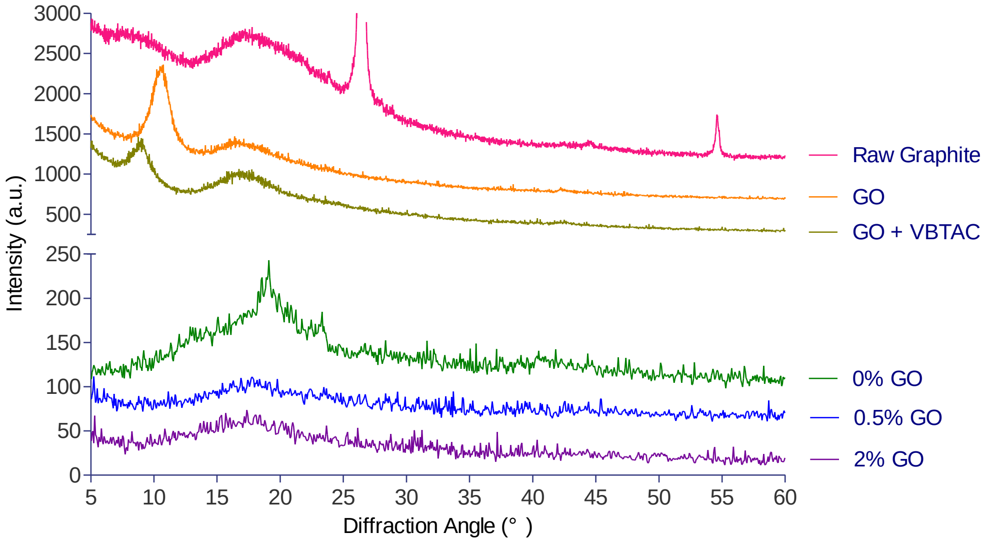

Figure 4. XRD spectra of raw graphite, GO, VBTAC-modified GO, GO/PMMA composites after miniemulsion with 0%, 0.5%, and 2% GO.

3.4. Thermal Stability Analysis

The thermal stability of raw graphite, GO, and VBTAC modified GO was analyzed by TGA (Figure 5). Raw graphite did not exhibit any weight loss below 600 °C, but about 8% of its weight was lost at 1000 °C. Regarding GO and VBTAC modified GO, approximate 10% weight loss was observed at 100 °C, which was attributed to the evaporation of water molecules trapped between the GO sheets due to the existence of many oxygen-containing functional groups on the GO galleries. An addition of 30% weight loss occurred between 150 °C and 250 °C, caused by the removal of the labile oxygen-containing functional groups [60-62]. In the temperature range from 300 °C to 1000 °C, GO and VBTAC modified GO lost another 10% and 25% of their weight, respectively. The 10% weight loss of GO could be attributed to the combustion of the exfoliated carbon skeleton of GO [63]. Furthermore, VBTAC modified GO had 15% more weight loss in comparison with that of GO between 300 °C to 1000 °C, which attributed the existence of the organic VBTAC. About 15 wt. % of VBTAC was loaded with GO together and it entered the GO galleries and bonded with GO sheets.

Peer-reviewed version available at J. Compos. Sci. 2020, 4, 118; doi:10.3390/jcs4030118

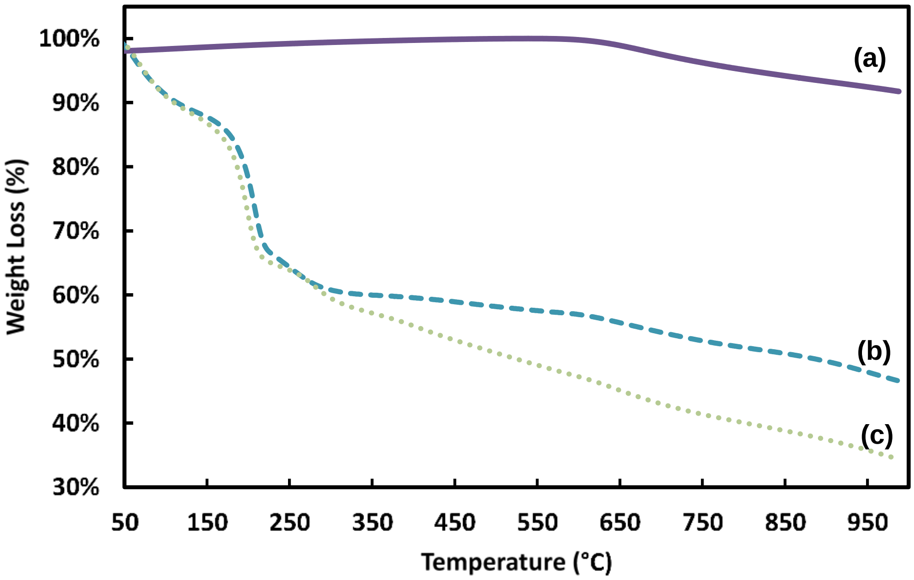

Figure 5. TGA thermograms of (a) raw graphite, (b) GO, and (c) VBTAC treated GO.

3.5. Particle Size Distribution of PMMA/GO Latex Droplets

During the miniemulsion polymerization process, we found that a stable miniemulsion of GO was difficult to prepare even though we had already chosen the optimized modifier for an organophilic GO (VBTAC modified GO). Compared with nanoclay, GO had higher density and smaller size, which may be the reason for its instability in the monomer phase. To increase the viscosity of the organophilic phase but avoid the disturbance to the polymerization kinetics when using the surfactants with the longer carbon chain (OTAB, MTAB) or the complicated structure (QAL), we used PVA to further stabilize the organophilic phase. PVA is a water-soluble synthetic polymer and has been applied for stabilizing emulsions and miniemulsions in combination with other surfactants or by itself. Specifically, when PVA was applied with other surfactants, the resulted latex showed better emulsion fluidity and stability and exhibited improved performance characteristics, such as excellent tackiness for adhesives, and better freeze-thaw stability [64-67]. PVA was used in our latex formulation to increase the viscosity for two reasons. First, higher viscosity providing by the PVA means the reduction in a collision between particles caused by mechanical processing, so that the particle size can be more precisely controlled. It is known that semi-vigorous agitation must be employed to suspend and disperse all nano-sized droplets, and the agitation could cause droplets to collide, merge and lose the encapsulated core during the miniemulsion formation and polymerization processes. Second, higher viscosity can help to stabilize the latex after polymerization, as shown in the latex stability study (Figure 8). Figure 6a showed that the average particle size decreased slightly with the increase of PVA content in the latex, which was similar to results obtained in previous studies [64-66]. Latex with 10% and 20% PVA had an average size of 250 and 230 nm, respectively. For latex with 0% and 5% PVA, a second peak representing the particles with the sizes of more than 4 μm appeared, resulting from the particle aggregation induced by the collision.

The GO loading affected the particle sizes of latex droplets as well. All experiments were carried out in triplicate. Analysis of variance (ANOVA) with Turkey test under a 95% confidence interval (a = 0.05) was used for statistical analysis. Figure 6b illustrated that the GO loading significantly increased the average particle sizes of latex droplets. To be more specific, the average particle size of PMMA without GO was about 200 nm. When the GO loading was increased to 0.25% and 0.5%, the particle size slightly increased to around 290 nm. This could be attributed to the encapsulation of GO particles inside the polymer droplets. In these cases, the thickness of the GO core was about 90 nm.

Peer-reviewed version available at *J. Compos. Sci.* **2020**, *4*, 118; doi:10.3390/jcs4030118

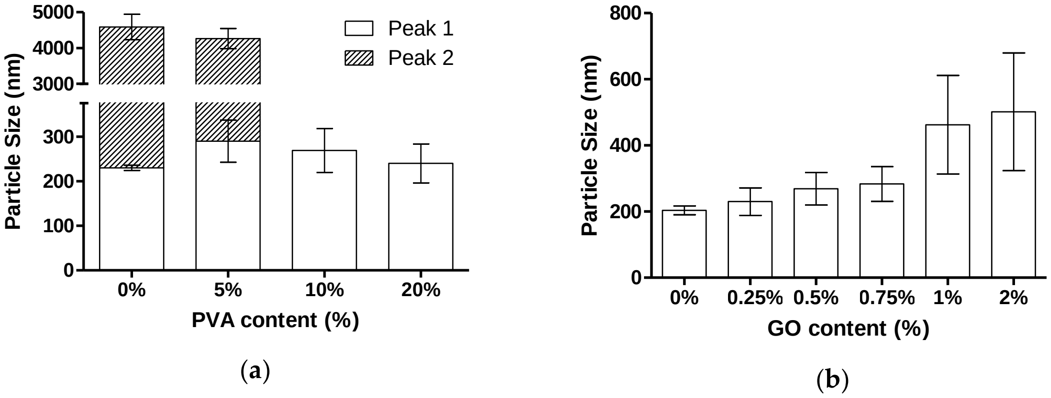

(**a**) (**b**)

Figure 6. Effect of a) the PVA loading (0.5% of GO), and b) the GO loading (10% PVA) on the particle sizes and size distribution of nanocomposite PMMA/GO latex prepared via miniemulsion polymerization.

When the GO loading increased to 0.75 % and 1%, the average particle size increased to about 400 and 480 nm, implying that GO aggregation occurred and some excessive GO could not be encapsulated by the polymer droplets. When the GO loading was increased to 2 %, the particle size increased to about 520 nm and further suggested that the aggregation formation of the excess GO particles. The particle size at the GO loading of 0.25 % and 0.5 % was very close, however, the particle size increased significantly when GO loading reached 0.75% and the excess and unencapsulated GO might exist in the system. In a higher GO loading (>0.5%), the formation of larger particle sizes and higher size dispersity may be explained as follows. Firstly, the encapsulation of more GO particles produced the larger composite droplets. Secondly, the “empty” polymer droplets were a lot smaller than droplets with GO inside, resulting in a large size dispersity. Thirdly, the GO sheets that were not encapsulated aggregated and formed large clusters. Thus, a GO loading of 0.5 % was chosen for further miniemulsion stability and morphology study.

3.6. Morphologies of GO, PMMA/GO latex and its melt films

Both SEM and TEM were used to measure the morphologies of the modified GO, PMMA/GO latex, and its melting films with or without the GO exfoliation. Figure 7a showed the structures of GO after VBTAC modification. The GO sheets with excellent transparency were overlapping together. This agreed well with the aforementioned XRD results, demonstrating that the increase of d-spacing between the GO galleries after oxidation and VBTAC intercalation. The size of the GO sheet was about 200-500 nm and the thickness was in the order of several nanometers. As shown in Figure 7b and 7c, the pure PMMA latex droplets, synthesized based on the basic recipe in Table 2, consisting of spherical particles with an average size of 200 nm and uniform size distribution.

Figure 7d and 7e illustrate the morphologies of nanocomposite latex in the presence of 0.5% VBTAC treated GO using the miniemulsion polymerization and encapsulation method. It was observed that the average particle size of PMMA/GO nanocomposite was approximately 250 nm. Some large particles with the particle size larger than 300 nm existed in the system as well. In the TEM image (Figure 7e), these large particles had dark cores representing the modified GO nanosheets inside the PMMA shell. Besides, the absence of un-encapsulated GO sheets, suggested that GO nanosheets were completely encapsulated by the PMMA shells. Figure 7f showed the melted film of this PMMA/GO nanocomposite film. GO nanoplatelets with several-nanometer thickness were seen in the polymer matrix, indicating the exfoliation and encapsulation of GO nanosheets after polymerization[68]. The VBTAC modification increased the interlayer spacing of GO and facilitated the intercalation of the monomer into the GO galleries. After that, the reaction of double bonds of the VBTAC located on the GO sheet and the monomer MMA during the polymerization process further facilitated the exfoliation of the polymer chain into the GO galleries.

To further confirm the effect of GO modified by the reactive modifier VBTAC, we conducted the same experiment using the GO without any modification. The morphologies of nanocomposite latex and its melting film prepared from the untreated GO (0.5%) was shown in Figure 7g, 7h, and 7i. Both SEM and TEM images (Figure 7g, 7h) clearly illustrated that the polymer/GO droplets formed the aggregates and only a few spherical particles were observed. Some flake shape particles with the size around 1μm existed, which could be the un-exfoliated or aggregated GO sheets. In Figure 7h, some aggregates of polymer droplets and dark "grainy" shaped GO clusters with a size about 1 μm were clearly shown in the TEM image. This result indicated that without the VBTAC treatment, the monomer was not able to cover or enter the galleries of the hydrophilic GO, which restrained both exfoliation and encapsulation of GO by the polymer particles during miniemulsion polymerization. Hydrophilic GO stayed in the water phase during the entire polymerization process. The image of the latex nanocomposite melting film (Figure 7i) revealed that the majority of GO sheets were not exfoliated and formed aggregated clusters dispersing in the polymer matrix. In summary,

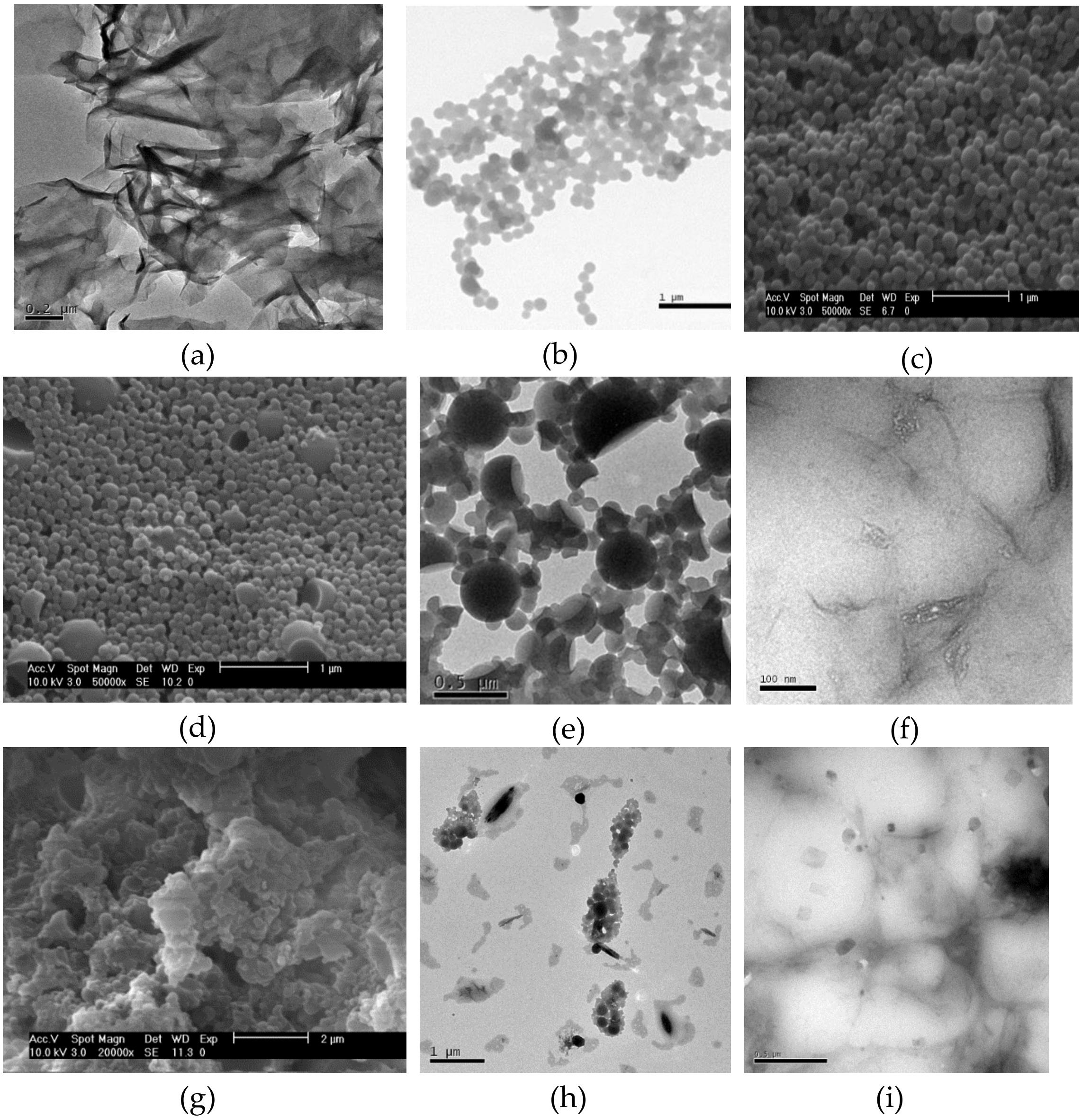

(a) (b) (c)

(d) (e) (f)

(g) (h) (i)

Figure 7. Images of a) TEM of VBTAC modified GO after sonication, b) SEM and c) TEM of neat PMMA nano-droplets; d) SEM and e) TEM of miniemulsions and f) TEM of the melted film of nanocomposites of the VBTAC modified GO (0.5%) encapsulated by PMMA; g) SEM and h) TEM of miniemulsions and i) TEM of the melted film of nanocomposites of untreated GO (0.5%) with PMMA.

Peer-reviewed version available at J. Compos. Sci. 2020, 4, 118; doi:10.3390/jcs4030118

the VBTAC modification was critical to form stable latex of the exfoliated and encapsulated PMMA/GO nanocomposite. The particle sizes of the nanocomposite droplets from these images agreed well with that from the DLS analysis.

3.7. Molecular Weight

The molecular weight (Mw, Mn) and the polydispersity index (PDI) of PMMA/GO nanocomposites with different VBTAC-modified GO loading levels were shown in Table 2. The molecular weight of the pure PMMA was about 130,000, which was comparable with the commercial grade PMMA (150,000, Sigma Aldrich). It denotes that miniemulsion polymerization is a viable method to synthesize high molecular weight polymer. The Mw of PMMA decreased with the addition of the modified GO. The existence of GO nanoparticles in the miniemulsion obstructed the growth of the polymer chain. Similar findings were observed in the miniemulsions of polymer encapsulated nanoclay composites [49, 69]. This was attributed to the irreversible reaction between the surface functional groups of the nanoclay and the growing radicals, where this reaction reduced radical concentration therefore directly affected the polymerization kinetics [49, 69]. But in this study, it was observed that with the increase of the modified GO loading from 1% to 2%, both Mw and PDI of nanocomposites were slightly higher than that of 0.5% of the modified GO. Our particle size analysis also provided some evidence that higher loading of GO might lead to some excess GO without encapsulation. The excess GO acted as the stabilizer for the miniemulsion and facilitated the polymerization reaction. The PDI increased with the GO loading, which agreed well with the polymer encapsulated nanoclay nanocomposite study. Nanoclay or nanodimensional GO in the miniemulsion disturbed the polymerization equilibrium and led to more chain transfer chances and the termination of propagation radicals [70, 71].

Table 2. The molecular weight of polymerized latex of PMMA with different GO loading levels.

	Mw	Mn	PDI
0% GO	1.28E+06	4.14E+05	3.11
0.5% GO	2.15E+05	4.49E+04	4.80
1% GO	2.99E+05	6.55E+04	4.57
2% GO	3.93E+05	6.14E+04	6.40

3.8. Stability of Latex

Figure 8 shows that the stability of latex varied at different GO loading and the PVA amount. Latex with 0.5 % VBTAC modified GO and 10% PVA (Figure 8 a) showed good stability over three months, no visible separation or sedimentation was observed. For comparison, the latex without any GO (Figure 8 g) but other similar formula had slight separation. This suggested that at an appropriate GO loading level, the exfoliated GO sheets were capable to effectively encapsulate by the polymer droplets, resulting in much more stable latex than that without GO. Further, when the GO loading increased from 0.5 % to 1% and 2%, the polymer droplets seemed to be easily separated from the aqueous phase and settled on the bottom. This might be due to the disturbance of the latex equilibrium caused by the aggregation of excessive GO nanoparticles as discussed previously. Figure 8d to 8f showed the effect of PVA percentage on the latex stability when the GO loading was kept at 0.5%. The increase in viscosity caused by the addition of PVA (from 5% to 20%) reduced the collision between composite particles, which was induced by mechanical processing. Mechanical agitation caused droplets to collide, merge, and lose the encapsulated core. The large black particles were shown in Figure 8 (d and e), indicating that the aggregation of the polymer/GO droplets was formed due to the mechanical collision when the PVA percentage was too low.

Peer-reviewed version available at *J. Compos. Sci.* **2020**, *4*, 118; doi:10.3390/jcs4030118

Figure 8. Stability of miniemulsion latex after sitting for more than 3 months. a) 0.5% GO, 10% PVA, b) 1% GO, 10% PVA, c) 2% GO, 10% PVA, d) 0.5% GO, 0% PVA, e) 0.5% GO, 5% PVA, f) 0.5% GO, 20% PVA, g) 0% GO, 10% PVA.

4. Discussion & Conclusion

The incompatibility between graphene or graphene oxide and the hydrophobic organic polymer impedes the development of the GO-based nanocomposites for their broad applications as energy, reinforced, and environmental materials. The dispersion of nano-dimensional graphene and GO plays a critical role in the final material properties such as percolation threshold, electric conductivity, and mechanical properties. In this study, different types of modifiers, including anionic surfactant, cationic quaternary ammonium with the reactive end group, and various carbon chains lengths or backbone structures, were used to optimize the organophilic GO to determine which was the best for the stability and reactivity within its monomeric medium. We found that among these modifiers, the VBTAC not only converted GO from hydrophilic to organophilic but also allowed the reactive end groups to further bind with the polymer together during the subsequent free radical miniemulsion polymerization process. A stable latex of the exfoliated PMMA encapsulated nano-dimensional GO composite was successfully synthesized using the VBTAC-modified GO with the addition of PVA. The addition of 10% PVA polymer played an important role in the latex stability by increasing viscosity to impede the mechanical collisions between the monomer and polymer encapsulated GO nanoparticles. The XRD and TEM and SEM images showed the exfoliation of polymer/GO nanocomposites. The uniform distribution of the exfoliated and nano-dimensional GO in the polymer matrix formed a stable latex with an average particle size of less than 300 nm with the ability to remain in solution for long-term storage. The next step in these studies is to determine a variety of other properties needed from this uniform distribution of exfoliated GO in the polymer nanocomposite for various applications.

Author Contributions: Conceptualization, Z.T., L.W., H.W; methodology, H.W, and L.W.; validation, Z.T., L.W. H.W., and M.C.; formal analysis, Z.T., L.W., F.W.; investigation, L.W., F.W., S. M.; data curation, L.W., F.W.; writing—original draft preparation, L.W, and F.W.; writing—review and editing, Z.T., F.W., S.M., H.L., M.C.; visualization, L.W and F.W.; supervision, Z.T.; project administration, Z.T.; funding acquisition, L.W, and Z.T. All authors have read and agreed to the published version of the manuscript.

Funding: This research received no external funding.

Acknowledgments: The authors thank the major research service center (RSC) staff at the University of Florida for the assistance of SEM, TEM, and XRD studies. The author also thanks the Chinese Scholarship Council (CSC) to provide financial support for F.W. to visit the USA. Partial funding was also provided for F.W. by the Hunan Provincial Key R&D Program of China (2017WK2022).

Peer-reviewed version available at *J. Compos. Sci.* **2020**, *4*, 118; doi:10.3390/jcs4030118

Conflicts of Interest: The authors declare no conflict of interest.

References

1. Moniruzzaman, M.; Winey, K. I., Polymer nanocomposites containing carbon nanotubes. *Macromolecules* **2006,** *39* (16).
2. Huang, J. C., Carbon black filled conducting polymers and polymer blends. *Advances in Polymer Technology: Journal of the Polymer Processing Institute* **2002,** *21* (4), 299-313.
3. Tong, Z.; Deng, Y., Synthesis of polystyrene encapsulated nanosaponite composite latex via miniemulsion polymerization. *Polymer* **2007,** *48* (15), 4337-4343.
4. Jairam, S.; Tong, Z.; Wang, L.; Welt, B., Encapsulation of a biobased lignin–saponite nanohybrid into polystyrene co-butyl acrylate (PSBA) latex via miniemulsion polymerization. *ACS Sustainable Chemistry & Engineering* **2013,** *1* (12), 1630-1637.
5. Choi, S.; Han, S. I.; Kim, D.; Hyeon, T.; Kim, D.-H., High-performance stretchable conductive nanocomposites: materials, processes, and device applications. *Chemical Society Reviews* **2019,** *48* (6), 1566-1595.
6. Liu, J.; Ma, Q.; Huang, Z.; Liu, G.; Zhang, H., Recent progress in graphene-based noble-metal nanocomposites for electrocatalytic applications. *Advanced Materials* **2019,** *31* (9), 1800696.
7. Farahani, R. D.; Dubé, M.; Therriault, D., Three-dimensional printing of multifunctional nanocomposites: manufacturing techniques and applications. *Advanced Materials* **2016,** *28* (28), 5794-5821.
8. Bhattacharya, S.; Samanta, S. K., Soft-nanocomposites of nanoparticles and nanocarbons with supramolecular and polymer gels and their applications. *Chemical reviews* **2016,** *116* (19), 11967-12028.
9. Boland, C. S.; Khan, U.; Ryan, G.; Barwich, S.; Charifou, R.; Harvey, A.; Backes, C.; Li, Z.; Ferreira, M. S.; Möbius, M. E., Sensitive electromechanical sensors using viscoelastic graphene-polymer nanocomposites. *Science* **2016,** *354* (6317), 1257-1260.
10. Lee, C.; Wei, X.; Kysar, J. W.; Hone, J., Measurement of the elastic properties and intrinsic strength of monolayer graphene. *science* **2008,** *321* (5887), 385-388.
11. Balandin, A. A.; Ghosh, S.; Bao, W.; Calizo, I.; Teweldebrhan, D.; Miao, F.; Lau, C. N., Superior thermal conductivity of single-layer graphene. *Nano letters* **2008,** *8* (3), 902-907.
12. Du, X.; Skachko, I.; Barker, A.; Andrei, E. Y., Approaching ballistic transport in suspended graphene. *Nature nanotechnology* **2008,** *3* (8), 491-495.
13. Bunch, J. S.; Verbridge, S. S.; Alden, J. S.; Van Der Zande, A. M.; Parpia, J. M.; Craighead, H. G.; McEuen, P. L., Impermeable atomic membranes from graphene sheets. *Nano letters* **2008,** *8* (8), 2458-2462.
14. Chang, H.; Wu, H., Graphene-based nanocomposites: preparation, functionalization, and energy and environmental applications. *Energy & Environmental Science* **2013,** *6* (12), 3483-3507.
15. Pei, S.; Wei, Q.; Huang, K.; Cheng, H.-M.; Ren, W., Green synthesis of graphene oxide by seconds timescale water electrolytic oxidation. *Nature communications* **2018,** *9* (1), 1-9.
16. Chen, J.; Zhang, Y.; Zhang, M.; Yao, B.; Li, Y.; Huang, L.; Li, C.; Shi, G., Water-enhanced oxidation of graphite to graphene oxide with controlled species of oxygenated groups. *Chemical science* **2016,** *7* (3), 1874-1881.
17. Shen, J.; Hu, Y.; Shi, M.; Lu, X.; Qin, C.; Li, C.; Ye, M., Fast and facile preparation of graphene oxide and reduced graphene oxide nanoplatelets. *Chemistry of Materials* **2009,** *21* (15), 3514-3520.
18. Kim, H.; Abdala, A. A.; Macosko, C. W., Graphene/polymer nanocomposites. *Macromolecules* **2010,** *43* (16), 6515-6530.

19. Etmimi, H. M.; Sanderson, R. D., New approach to the synthesis of exfoliated polymer/graphite nanocomposites by miniemulsion polymerization using functionalized graphene. *Macromolecules* **2011,** *44* (21), 8504-8515.

20. Putz, K. W.; Compton, O. C.; Palmeri, M. J.; Nguyen, S. T.; Brinson, L. C., High-nanofiller-content graphene oxide–polymer nanocomposites via vacuum-assisted self-assembly. *Advanced Functional Materials* **2010,** *20* (19), 3322-3329.

21. Xing, J.; Deng, B.; Liu, Q., Effect of graphene nanoplatelets on the performance of polyphenylene sulfide composites produced by melt intercalation. *High Performance Polymers* **2018,** *30* (5), 519-526.

22. Bijarimi, M.; Amirul, M.; Norazmi, M.; Ramli, A.; Desa, M. S. Z.; Desa, M. D. A.; Samah, M. A. A., Preparation and characterization of poly (lactic acid)(PLA)/polyamide 6 (PA6)/graphene nanoplatelet (GNP) blends bio-based nanocomposites. *Materials Research Express* **2019,** *6* (5), 055044.

23. Mishra, S. K.; Tripathi, S. N.; Choudhary, V.; Gupta, B. D., Surface plasmon resonance-based fiber optic methane gas sensor utilizing graphene-carbon nanotubes-poly (methyl methacrylate) hybrid nanocomposite. *Plasmonics* **2015,** *10* (5), 1147-1157.

24. Rajabi, M.; Mahanpoor, K.; Moradi, O., Preparation of PMMA/GO and PMMA/GO-Fe3O4 nanocomposites for malachite green dye adsorption: Kinetic and thermodynamic studies. *Composites Part B: Engineering* **2019,** *167*, 544-555.

25. Thomassin, J.-M.; Trifkovic, M.; Alkarmo, W.; Detrembleur, C.; Jérôme, C.; Macosko, C., Poly (methyl methacrylate)/graphene oxide nanocomposites by a precipitation polymerization process and their dielectric and rheological characterization. *Macromolecules* **2014,** *47* (6), 2149-2155.

26. Wang, W.-P.; Pan, C.-Y., Preparation and characterization of polystyrene/graphite composite prepared by cationic grafting polymerization. *Polymer* **2004,** *45* (12), 3987-3995.

27. Hu, H.; Wang, X.; Wang, J.; Wan, L.; Liu, F.; Zheng, H.; Chen, R.; Xu, C., Preparation and properties of graphene nanosheets–polystyrene nanocomposites via in situ emulsion polymerization. *Chemical Physics Letters* **2010,** *484* (4-6), 247-253.

28. Poddar, M. K.; Pradhan, S.; Moholkar, V. S.; Arjmand, M.; Sundararaj, U., Ultrasound–assisted synthesis and characterization of polymethyl methacrylate/reduced graphene oxide nanocomposites. *AIChE Journal* **2018,** *64* (2), 673-687.

29. Fadil, Y.; Agarwal, V.; Jasinski, F.; Thickett, S. C.; Minami, H.; Zetterlund, P. B., Electrically conductive polymer/rGO nanocomposite films at ambient temperature via miniemulsion polymerization using GO as surfactant. *Nanoscale* **2019,** *11* (14), 6566-6570.

30. Zhang, L.; Yang, W.; Jiang, Z.; He, F.; Zhang, K.; Fan, J.; Wu, J., Graphene oxide-modified microencapsulated phase change materials with high encapsulation capacity and enhanced leakage-prevention performance. *Applied Energy* **2017,** *197*, 354-363.

31. Thickett, S. C.; Wood, N.; Ng, Y. H.; Zetterlund, P. B., Hollow hybrid polymer–graphene oxide nanoparticles via Pickering miniemulsion polymerization. *Nanoscale* **2014,** *6* (15), 8590-8594.

32. Huynh, V. T.; Nguyen, D.; Such, C. H.; Hawkett, B. S., Polymer coating of graphene oxide via reversible addition–fragmentation chain transfer mediated emulsion polymerization. *Journal of Polymer Science Part A: Polymer Chemistry* **2015,** *53* (12), 1413-1421.

33. Pham, V. H.; Dang, T. T.; Hur, S. H.; Kim, E. J.; Chung, J. S., Highly conductive poly (methyl methacrylate)(PMMA)-reduced graphene oxide composite prepared by self-assembly of PMMA latex and graphene oxide through electrostatic interaction. *ACS applied materials & interfaces* **2012,** *4* (5), 2630-2636.

34. Pham, V. H.; Dang, T. T.; Hur, S. H.; Kim, E. J.; Chung, J. S., Highly Conductive Poly(methyl methacrylate) (PMMA)-Reduced Graphene Oxide Composite Prepared by Self-Assembly of PMMA Latex and Graphene Oxide through Electrostatic Interaction. *ACS Applied Materials & Interfaces* **2012,** *4* (5), 2630-2636.

35. Pan, G.; Sudol, E. D.; Dimonie, V. L.; El-Aasser, M. S., Nitroxide-mediated living free radical miniemulsion polymerization of styrene. *Macromolecules* **2001,** *34* (3), 481-488.

36. Taden, A.; Landfester, K., Crystallization of poly (ethylene oxide) confined in miniemulsion droplets. *Macromolecules* **2003,** *36* (11), 4037-4041.

37. Schork, F. J.; Luo, Y.; Smulders, W.; Russum, J. P.; Butté, A.; Fontenot, K., Miniemulsion polymerization. In *Polymer particles*, Springer: 2005; pp 129-255.

38. Asua, J. M., Miniemulsion polymerization. *Progress in polymer science* **2002,** *27* (7), 1283-1346.

39. Che Man, S.; Thickett, S. C.; Whittaker, M. R.; Zetterlund, P. B., Synthesis of polystyrene nanoparticles “armoured” with nanodimensional graphene oxide sheets by miniemulsion polymerization. *Journal of Polymer Science Part A: Polymer Chemistry* **2013,** *51* (1), 47-58.

40. Che Man, S.; Mohd Yusof, N.; Whittaker, M. R.; Thickett, S. C.; Zetterlund, P. B., Influence of monomer type on miniemulsion polymerization systems stabilized by graphene oxide as sole surfactant. *Journal of Polymer Science Part A: Polymer Chemistry* **2013,** *51* (23), 5153-5162.

41. Teo, G. H.; Ng, Y. H.; Zetterlund, P. B.; Thickett, S. C., Factors influencing the preparation of hollow polymer-graphene oxide microcapsules via Pickering miniemulsion polymerization. *Polymer* **2015,** *63*, 1-9.

42. Tokuda, M.; Yamane, M.; Thickett, S. C.; Minami, H.; Zetterlund, P. B., Synthesis of polymeric nanoparticles containing reduced graphene oxide nanosheets stabilized by poly (ionic liquid) using miniemulsion polymerization. *Soft matter* **2016,** *12* (17), 3955-3962.

43. Tan, Y.; Fang, L.; Xiao, J.; Song, Y.; Zheng, Q., Grafting of copolymers onto graphene by miniemulsion polymerization for conductive polymer composites: improved electrical conductivity and compatibility induced by interfacial distribution of graphene. *Polymer Chemistry* **2013,** *4* (10), 2939-2944.

44. Fadil, Y.; Jasinski, F.; Guok, T. W.; Thickett, S. C.; Minami, H.; Zetterlund, P. B., Pickering miniemulsion polymerization using graphene oxide: effect of addition of a conventional surfactant. *Polymer Chemistry* **2018,** *9* (24), 3368-3378.

45. Man, S. C.; Ly, D.; Whittaker, M. R.; Thickett, S. C.; Zetterlund, P. B., Nano-sized graphene oxide as sole surfactant in miniemulsion polymerization for nanocomposite synthesis: Effect of pH and ionic strength. *Polymer* **2014,** *55* (16), 3490-3497.

46. Hummers Jr, W. S.; Offeman, R. E., Preparation of graphitic oxide. *Journal of the american chemical society* **1958,** *80* (6), 1339-1339.

47. Ten, E.; Vermerris, W., Recent developments in polymers derived from industrial lignin. *Journal of Applied Polymer Science* **2015,** *132* (24).

48. Jairam, S.; Tong, Z.; Wang, L.; Welt, B., Encapsulation of a Biobased Lignin-Saponite Nanohybrid into Polystyrene Co-Butyl Acrylate (PSBA) Latex via Miniemulsion Polymerization. *Acs Sustainable Chemistry & Engineering* **2013,** *1* (12), 1630-1637.

49. Zhong, Y.; Zhu, Z.; Wang, S.-Q., Synthesis and rheological properties of polystyrene/layered silicate nanocomposite. *Polymer* **2005,** *46* (9), 3006-3013.

50. Deraguin, B. V.; Landau, L., Theory of the stability of strongly charged lyophobic sols and of the adhesion of strongly charged particles in solution of electrolytes. *Acta Physicochim: USSR* **1941,** *14*, 633-662.

51. Verwey, E. J. W., Theory of the stability of lyophobic colloids. *The Journal of Physical Chemistry* **1947,** *51* (3), 631-636.

Peer-reviewed version available at J. Compos. Sci. 2020, 4, 118; doi:10.3390/jcs4030118

52. Liu, H.; Zhang, L.; Guo, Y.; Cheng, C.; Yang, L.; Jiang, L.; Yu, G.; Hu, W.; Liu, Y.; Zhu, D., Reduction of graphene oxide to highly conductive graphene by Lawesson's reagent and its electrical applications. *Journal of Materials Chemistry C* **2013,** *1* (18), 3104-3109.

53. Zangmeister, C. D., Preparation and evaluation of graphite oxide reduced at 220 C. *Chemistry of Materials* **2010,** *22* (19), 5625-5629.

54. Nethravathi, C.; Rajamathi, M., Chemically modified graphene sheets produced by the solvothermal reduction of colloidal dispersions of graphite oxide. *Carbon* **2008,** *46* (14), 1994-1998.

55. Titelman, G. I.; Gelman, V.; Bron, S.; Khalfin, R. L.; Cohen, Y.; Bianco-Peled, H., Characteristics and microstructure of aqueous colloidal dispersions of graphite oxide. *Carbon* **2005,** *43* (3), 641-649.

56. Uhl, F. M.; Yao, Q.; Nakajima, H.; Manias, E.; Wilkie, C. A., Expandable graphite/polyamide-6 nanocomposites. *Polymer Degradation and Stability* **2005,** *89* (1), 70-84.

57. Park, S.; An, J.; Potts, J. R.; Velamakanni, A.; Murali, S.; Ruoff, R. S., Hydrazine-reduction of graphite- and graphene oxide. *carbon* **2011,** *49* (9), 3019-3023.

58. Khezri, K.; Haddadi-Asl, V.; Roghani-Mamaqani, H.; Salami-Kalajahi, M., Encapsulation of organomodified montmorillonite with PMMA via in situ SR&NI ATRP in miniemulsion. *Journal of Polymer Research* **2012,** *19* (5), 9868.

59. Lan, F.; Liu, K.-X.; Jiang, W.; Zeng, X.-B.; Wu, Y.; Gu, Z.-W., Facile synthesis of monodisperse superparamagnetic Fe3O4/PMMA composite nanospheres with high magnetization. *Nanotechnology* **2011,** *22* (22), 225604.

60. Li, C.; Wang, X.; Liu, Y.; Wang, W.; Wynn, J.; Gao, J., Using glucosamine as a reductant to prepare reduced graphene oxide and its nanocomposites with metal nanoparticles. *Journal of Nanoparticle Research* **2012,** *14* (6), 875.

61. Wu, T.; Wang, X.; Qiu, H.; Gao, J.; Wang, W.; Liu, Y., Graphene oxide reduced and modified by soft nanoparticles and its catalysis of the Knoevenagel condensation. *Journal of Materials Chemistry* **2012,** *22* (11), 4772-4779.

62. Wang, X.; Wen, X.; Liu, Z.; Tan, Y.; Yuan, Y.; Zhang, P., Rapid and efficient synthesis of soluble graphene nanosheets using N-methyl-p-aminophenol sulfate as a reducing agent. *Nanotechnology* **2012,** *23* (48), 485604.

63. Wang, P.; Tang, Y.; Dong, Z.; Chen, Z.; Lim, T.-T., Ag–AgBr/TiO 2/RGO nanocomposite for visible-light photocatalytic degradation of penicillin G. *Journal of Materials Chemistry A* **2013,** *1* (15), 4718-4727.

64. Kim, N.; Sudol, E. D.; Dimonie, V. L.; El-Aasser, M. S., Poly (vinyl alcohol) stabilization of acrylic emulsion polymers using the miniemulsion approach. *Macromolecules* **2003,** *36* (15), 5573-5579.

65. Kim, N.; Sudol, E. D.; Dimonie, V. L.; El-Aasser, M. S., Comparison of conventional and miniemulsion copolymerizations of acrylic monomers using poly (vinyl alcohol) as the sole stabilizer. *Macromolecules* **2004,** *37* (7), 2427-2433.

66. Yuki, K.; Nakamae, M.; Sato, T.; Maruyama, H.; Okaya, T., Physical properties of acrylic copolymer emulsions using poly (vinyl alcohol) as a protective colloid in comparison with those using surfactants. *Polymer international* **2000,** *49* (12), 1629-1635.

67. Robeson, L. M.; Vratsanos, M. S. In *Mechanical characterization of vinyl acetate based emulsion polymer blends*, 2000; Wiley Online Library: pp 117-138.

68. Choi, K. S.; Liu, F.; Choi, J. S.; Seo, T. S., Fabrication of free-standing multilayered graphene and poly (3, 4-ethylenedioxythiophene) composite films with enhanced conductive and mechanical properties. *Langmuir* **2010,** *26* (15), 12902-12908.

Peer-reviewed version available at *J. Compos. Sci.* **2020**, *4*, 118; doi:10.3390/jcs4030118

69. Samakande, A.; Sanderson, R. D.; Hartmann, P. C., Encapsulated clay particles in polystyrene by RAFT mediated miniemulsion polymerization. *Journal of Polymer Science Part A: Polymer Chemistry* **2008,** *46* (21), 7114-7126.

70. Tong, Z.; Deng, Y., Kinetics of miniemulsion polymerization of styrene in the presence of organoclays. *Macromolecular Materials and Engineering* **2008,** *293* (6), 529-537.

71. Roghani-Mamaqani, H.; Haddadi-Asl, V.; Najafi, M.; Salami-Kalajahi, M., Preparation of tailor-made polystyrene nanocomposite with mixed clay-anchored and free chains via atom transfer radical polymerization. *AIChE Journal* **2011,** *57* (7), 1873-1881.